Control of the Bridgehead Donor Atom in the Tripodal Ligand over Oxidative Addition of $Au(PPh_3)^+$ to $[X(CH_2CH_2PPh_2)_3RhH]$ (X = N, P). X-ray Diffraction and Multinuclear (^{103}Rh, ^{31}P, ^1H) NMR Studies

Claudio Bianchini,*[1a] Cornelis J. Elsevier,[1b] Jan M. Ernsting,[1b] Maurizio Peruzzini,[1a] and Fabrizio Zanobini[1a]

Istituto per lo Studio della Stereochimica ed Energetica dei Composti di Coordinazione del CNR, Via J. Nardi 39, I-50132 Florence, Italy, and Anorganisch Chemisch Laboratorium, van't Hoff Research Institute, Universiteit van Amsterdam, Nieuwe Achtergracht 166, 1018 WV Amsterdam, The Netherlands

Received June 17, 1994[⊗]

The electrophilic fragment $Au(PPh_3)^+$ reacts in tetrahydrofuran with the monohydrides $[(NP_3)RhH]$ and $[(PP_3)RhH]$ to give the mixed-metal adducts $[(NP_3)Rh(H)\{Au(PPh_3)\}]^+$ and $[(PP_3)Rh(\mu\text{-}H)\{Au(PPh_3)\}]^+$, respectively [$NP_3 = N(CH_2CH_2PPh_2)_3$; $PP_3 = P(CH_2CH_2PPh_2)_3$]. The structures of $[(NP_3)Rh(H)\{Au(PPh_3)\}]PF_6 \cdot 0.5C_4H_8O$ (**4**) and of $[(PP_3)Rh(\mu\text{-}H)\{Au(PPh_3)\}]BPh_4 \cdot 0.5C_2H_5OH$ (**3b**) have been determined by X-ray diffraction analyses. Compound **4** crystallizes in monoclinic space group P21/*c* (No. 14) with $a = 11.132(4)$ Å, $b = 20.779(4)$ Å, $c = 26.647(5)$ Å, $\beta = 97.63(1)°$, $Z = 4$, and $V = 6105.71$ Å^3. The rhodium(III) center is coordinated in a distorted octahedral geometry by the nitrogen and the three phosphorus atoms of NP_3, by a gold atom from $Au(PPh_3)$, *trans* to nitrogen, and by a terminal hydride ligand. The Rh-Au distance in **4** [2.531(1) Å] is the shortest ever reported. Compound **3b** crystallizes in monoclinic space group P21/*a* (No. 14) with $a = 14.775(4)$ Å, $b = 35.627(4)$ Å, $c = 14.113(4)$ Å, $\beta = 95.94(5)°$, $Z = 4$, and $V = 7389.04$ Å^3. The geometry of the coordination polyhedron around rhodium approximates a trigonal bipyramid with the bridgehead phosphorus and an intact $HAu(PPh_3)$ group *transoid* to each other. All the mixed rhodium-gold hydrides have been studied in solution by means of NMR techniques, including ^{103}Rh spectra obtained from inverse $^1H,\{^{103}Rh\}$ experiments. These studies confirm that, also in solution, the presence of nitrogen in the tripodal ligand results in oxidative addition of $Au(PPh_3)^+$ to the metal, whereas formal oxidation of the terminal hydride occurs when the bridgehead donor atom is phosphorus.

Introduction

Oxidative addition reactions of various inorganic and organic electrophiles to either $[(tripod)M]^+$ fragments or neutral [(tripod)ML] complexes have extensively been investigated in recent years [tripod = $N(CH_2CH_2PPh_2)_3$, $P(CH_2CH_2PPh_2)_3$; L = uninegative ligand; M = Co, Rh, Ir].[2-5]

Given the presence of four donor atoms and the equivalence of the three arms departing from the bridgehead nitrogen or phosphorus atoms, the tripodal ligands $N(CH_2CH_2PPh_2)_3$ (NP_3) and $P(CH_2CH_2PPh_2)_3$ (PP_3) wrap d^8 metal ions in an umbrella-like fashion (**I**). As a consequence of oxidative addition of an

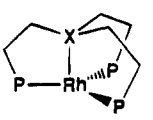

I

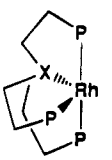

II

X = N, P

L-L′ substrate, the former trigonal-pyramidal (tripod)M fragment is invariably transformed into a d^6-metal butterfly fragment (pseudo C_{2v} symmetry) more or less distorted depending on the steric and electronic requirements of the coligands (**II**).[6]

It is generally observed that the propensity of the resulting octahedral $[(tripod)MLL']^+$ complexes to undergo the eventual reductive elimination of the L-L′ molecule is lower for NP_3 complexes than for analogous PP_3 derivatives. Some representative examples of this phenomenon are the followings. The NP_3 complexes $[(NP_3)Rh(H)_2]BPh_4$,[5] $[(NP_3)M(H)(CO_2Et)]BPh_4$ (M = Rh,[3a] Ir[7]) and $[(NP_3)Rh(H)(COMe)]BPh_4$[3f] are stable and isolable species at room temperature, whereas the PP_3 analogs more or less rapidly eliminate H_2, ethanol, and acetaldehyde, respectively.[3a-c,5,7]

[⊗] Abstract published in *Advance ACS Abstracts,* November 15, 1994.

(1) (a) ISSECC, CNR, Florence. (b) van't Hoff Laboratorium, Amsterdam.

(2) (a) Bianchini, C.; Mealli, C.; Meli, A.; Peruzzini, M.; Zanobini, F. *J. Am. Chem. Soc.* **1988**, *110*, 8725. (b) Bianchini, C.; Innocenti, P.; Meli, A.; Peruzzini, M.; Vacca, A.; Zanobini, F. *Organometallics*, **1988**, *9*, 2514. (c) Bianchini, C.; Peruzzini, M.; Vacca, A.; Zanobini F. *Organometallics* **1991**, *10*, 3697. (d) Bianchini, C.; Peruzzini, M.; Zanobini, F. *Organometallics* **1991**, *10*, 3415. (e) Bianchini, C.; Mealli, C.; Peruzzini, M.; Zanobini, F. *J. Am. Chem. Soc.* **1992**, *114*, 5905.

(3) (a) Bianchini, C.; Peruzzini, M.; Vizza, F.; Zanobini, F. *J. Organomet. Chem.* **1988**, *346*, C9. (b) Bianchini, C.; Meli, A.; Peruzzini, M.; Vacca, A., Zanobini, F. *Organometallics* **1987**, *6*, 2453. (c) Bianchini, C.; Meli, A.; Peruzzini, M.; Ramirez, J. A.; Vacca, A.; Vizza, F.; Zanobini, F. *Organometallics* **1989**, *8*, 337. (d) Bianchini, C.; Laschi, F.; Ottaviani, M. F.; Peruzzini, M.; Zanello, P.; Zanobini, F. *Organometallics* **1989**, *8*, 893. (e) Bianchini, C.; Masi, D.; Peruzzini, M.; Ramirez, J. A.; Vacca, A.; Zanobini, F. *Organometallics* **1989**, *8*, 2179. (f) Bianchini, C.; Meli, A.; Peruzzini, M.; Vizza, F.; Bachechi, F. *Organometallics* **1991**, *10*, 820. (g) Di Vaira, M.; Rovai, D.; Stoppioni, P.; Peruzzini, M. *J. Organomet. Chem.* **1991**, *420*, 135. (h) Bianchini, C.; Masi, D.; Mealli, C.; Meli, A.; Sabat, M. *Organometallics* **1985**, *4*, 1014.

(4) (a) Bianchini, C.; Masi, D.; Meli, A.; Peruzzini, M.; Sabat, M.; Zanobini, F. *Organometallics* **1986**, *5*, 2557. (b) Bianchini, C.; Peruzzini, M.; Zanobini, F. *J. Organomet. Chem.* **1987**, *326*, C79.

(5) (a) Bianchini, C.; Mealli, C.; Peruzzini, M.; Zanobini, F. *J. Am. Chem. Soc.* **1987**, *109*, 5548. (b) Bianchini, C.; Masi, D.; Meli, A.; Peruzzini, M.; Zanobini, F. *J. Am. Chem. Soc.* **1988**, *110*, 6411.

(6) Mealli, C.; Ghilardi, C. A.; Orlandini, A. *Coord. Chem. Rev.* **1992**, *120*, 361.

(7) Bianchini, C.; Peruzzini, M. Unpublished results.

0020-1669/95/1334-0084$09.00/0

Table 1. Selected NMR Spectral Data for the Complexes

			$^{31}P\{^1H\}$[a]		^1H[b]		
compd	temp, °C	pattern	chem shift (multp)[d]	coupling const[g]	chem shift (multp)[d]	coupling const[g]	^{103}Rh[c]
1	20	AM_3X	$\delta(P_A)$ 158.88 (dq) $\delta(P_M)$ 63.99 (dd)	$J_{P_AP_M}$ 19.2 J_{P_ARh} 88.5 J_{P_MRh} 162.0	δ(RhH) −6.56 (dq)	J_{HP_A} 130.0 J_{HP_M} 17.0 J_{HRh} 17.0	−58[h]
2	20	A_3X	δ(P) 39.59 (d)	J_{PRh} 174.9	δ(RhH) −17.90 (q)	J_{HP} 24.2 J_{HRh} 24.2	−266[h]
3a,b[h]	21	AM_3QX[e]	$\delta(P_A)$ 161.06 (ddq) $\delta(P_M)$ 67.55 (ddd) $\delta(P_Q)$ 47.60 (dtd)	$J_{P_AP_M}$ 20.7 $J_{P_AP_Q}$ 46.7 J_{P_MPQ} 14.2 J_{P_ARh} 104.6 J_{P_MRh} 136.3 J_{P_QRh} 8.7	δ(RhHAu) −3.74 (dddq)	J_{HP_A} 84.3 J_{HP_M} 3.9 J_{HP_Q} 50.9 J_{HRh} 17.8	−1159[h]
4[h]	21	A_3MX[f]	$\delta(P_A)$ 46.51 (d) $\delta(P_M)$ 33.50 (d)	$J_{P_AP_M}$ ~0 J_{P_ARh} 119.6 J_{P_MRh} 11.7	δ(RhH) −9.44 (qdd)	J_{HP_A} 32.3 J_{HP_M} 5.6 J_{HRh} 14.1	−487

[a] All the proton-decoupled ^{31}P NMR spectra were recorded at 121.42 or 81.01 MHz in acetone-d_6 unless otherwise stated. The $^{31}P\{^1H\}$ NMR spectra of **3a** and **4** exhibit the high-field resonance due to the PF_6 counteranion [δ −145.5, septet, $^1J_{PF}$ 707.5 Hz]. [b] All ^1H NMR spectra were recorded at 299.94 or 200.13 MHz in acetone-d_6 unless otherwise stated. The resonances due to the hydrogen atoms of the PP_3 and NP_3 ligands and of the gold-bonded PPh_3 ligand are not reported. [c] All ^{103}Rh NMR spectra were recorded at 100.13 MHz by inverse ^1H, $\{^{103}Rh\}$ NMR spectroscopy at 30 °C. [d] Key: d, doublet, t, triplet, q, quartet. [e] The letter Q denotes the P atom of the triphenylphosphine ligand. [f] The letter M denotes the P atom of the triphenylphosphine ligand. [g] Coupling constants (J) are in hertz. [h] In dichloromethane-d_2.

On theoretical grounds, the different aptitude of NP_3 and PP_3 metal complexes to undergo reductive elimination/oxidative addition reaction sequences has recently been interpreted in terms of the different bond strength of the central donor atom in the tripods.[6] In particular, it has been proposed that larger geometrical distortions (and therefore higher energies) are required for $(PP_3)M$ fragments to develop the hybridized σ and π FMOs that promote the oxidative addition.

The question is not of fundamental relevance only as several PP_3 complexes with the metals of the cobalt triad efficiently catalyze a variety of homogeneous reactions,[2ab,3,8,10] whereas a few NP_3 complexes behave as homogeneous catalysts or catalyst precursors.[9,10]

Herein we report a study of the reactions between the trigonal-bipyramidal Rh(I) hydrides $[(NP_3)RhH]$ (**1**) and $[(PP_3)RhH]$ (**2**) and the electrophilic $Au(PPh_3)^+$ fragment. In view of the isolobal analogy between H^+ and $Au(PPh_3)^+$ units,[11] this work is also related to previous studies on the reactions of **1** and **2** with protic acids to give Rh(III) dihydrides of different stability.[5] In fact, while the classical dihydride structure is firmly maintained in solution by the NP_3 complex, the PP_3 derivative readily eliminates dihydrogen at room temperature.

Experimental Section

General Data. Reagent grade chemicals were used in the preparations of the complexes. Tetrahydrofuran (THF) was purified by distillation over $LiAlH_4$ under nitrogen just prior to use. Deuterated solvents for NMR measurements (Janssen and Aldrich) were dried over molecular sieves. Literature methods were used for the preparation of $[(PP_3)RhH]$ (**1**),[5b] $[(NP_3)RhH]$ (**2**),[5b] and $[AuCl(PPh_3)]$.[12] Infrared spectra were recorded on a Perkin-Elmer Series 1600 FTIR spectrophotometer using samples mulled in Nujol between KBr plates. Conductivities were measured with an Orion Model 990101 conductance cell connected to a Model 101 conductivity meter. The conductivity data were obtained at sample concentrations of *ca.* 1×10^{-3} M in nitroethane solutions at room temperature (21 °C). NMR spectra were recorded on Varian VXR 300 or Bruker AC 200P instruments operating at 299.94 and 200.13 MHz (^1H) and at 121.42 and 81.01 MHz (^{31}P), respectively. Peak positions are relative to tetramethylsilane as an external reference (^1H) or to external 85% H_3PO_4 ($^{31}P\{^1H\}$) with downfield values reported as positive. Proton NMR spectra with broad band and selective decoupling of the ^{31}P resonances were recorded on the Bruker AC 200P instrument equipped with a 5 mm inverse probe and a BFX-5 Bruker amplifier device using the wide band phosphorus decoupling sequence GARP. The spin-lattice relaxation times (T_1) were measured at 299.94 MHz with the inversion−recovery sequence in CD_2Cl_2.

^{103}Rh NMR spectra. The inverse $^1H,\{^{103}Rh\}$ NMR experiments were performed similarly to previous studies where this technique has been employed[13] and were carried out on a Bruker AC 100 spectrometer provided with an "inverse modification" operating at 2.35 T, a 10-mm $^{103}Rh/^{31}P/^1H$ probe, a second PTS 160 frequency synthesizer with 90° phase shift capability, and a BSV-3 heteronucleus decoupler provided with an 80 W selective ^{103}Rh amplifier. The sequence as provided by Bax *et al.*[14] was used. A typical procedure is as follows. A CD_2Cl_2 solution of *ca.* 3×10^{-2} M was used for each complex. After a first experiment with low resolution, a more accurate measurement was performed with a slightly altered carrier offset. The 90° ^1H pulse was 30.5 μs, the 90° ^{103}Rh pulse amounted to 40 μs, and the 1/2J period was set at 28 ms. The total experimental time was *ca.* 8 h. The 512 × 2048 matrix was zerofilled in F_1 and a sine-squared weighing was applied prior to the double Fourier transform, giving a resolution better than 2 Hz (< 1 ppm) in the ^{103}Rh domain. Calculation of $\delta(^{103}Rh)$ was carried out by determining the absolute ^{103}Rh frequency of the cross peak and relating it to the arbitrary frequency (Ξ = 3.16 MHz) scaled for the operating field (100.13 MHz). Signals at higher field are taken as negative chemical shifts.

Synthesis of the Complexes. All reactions and manipulations were routinely performed under nitrogen, unless otherwise stated, by using Schlenk-tube techniques. The solid complexes were collected on sintered-glass frits and washed with ethanol and petroleum ether (bp 40−70 °C) before being dried under a stream of nitrogen.

The reactions described in this paper are summarized in Scheme 1. Selected ^1H, $^{31}P\{^1H\}$, and ^{103}Rh NMR spectral data for the complexes are reported in Table 1.

(8) Bianchini, C.; Meli, A; Peruzzini, M.; Vizza, F.; Zanobini, F. *Coord. Chem. Rev.* **1992**, *120*, 193.
(9) Bianchini, C.; Meli, A.; Peruzzini, M.; Zanobini, F.; Bruneau, C.; Dixneuf, P. H. *Organometallics* **1990**, *9*, 1155.
(10) Bianchini, C.; Meli, A; Peruzzini, M.; Vizza, F. *Organometallics* **1990**, *9*, 1146.
(11) (a) Hoffmann, R. *Angew. Chem., Int. Ed. Engl.* **1982**, *21*, 711. (b) Stone, F. G. A. *Angew. Chem., Int. Ed. Engl.* **1984**, *23*, 89.
(12) Bruce, M. I.; Nicholson, B. K.; Bin Shawkataly, O. *Inorg. Synth.* **1989**, *26*, 325.
(13) (a) Benn, R.; Brenneke, H.; Rufinska, A. *J. Organomet. Chem.* **1987**, *320*, 115. (b) H. van der Zeijden, A. A.; van Koten, G.; Ernsting, J. M.; Elsevier, C. J. *J. Chem. Soc., Dalton Trans.* **1989**, 317. (c) Bucher, U. E.; Lengweiler, T.; Nanz, D.; von Philipsborn, W.; Venanzi, L. M. *Angew. Chem. Int. Ed. Engl.* **1990**, *29*, 548. (d) Ceccon A.; Elsevier, C. J.; Ernsting, J. M.; Santi, S.; Venzo, A. *Inorg. Chim. Acta* **1993**, *204*, 15.
(14) Bax, A.; Griffey, R. H.; Hawkins, B. L. *J. Magn. Reson.* **1983**, *55*, 301.

Table 2. Experimental Data for the X-ray Diffraction Study of $[(PP_3)Rh(\mu\text{-}H)\{Au(PPh_3)\}]BPh_4 \cdot 0.5C_2H_5OH$ (**3b**) and $[(NP_3)Rh(H)\{Au(PPh_3)\}]PF_6 \cdot 0.5C_4H_8O$ (**4**)

	3b	**4**
chem formula	$C_{85}H_{78}AuBO_{0.5}P_5Rh$	$C_{62}H_{62}AuF_6NO_{0.5}P_5Rh$
mol wt	1573.09	1397.95
cryst system	monoclinic	monoclinic
space group	*P*21/*a* (No. 14)	*P*21/*c* (No. 14)
a, Å	14.775(4)	11.132(4)
b, Å	35.627(4)	20.779(4)
c, Å	14.113(4)	26.647(5)
b, deg	95.94(5)	97.63(1)
Z	4	4
V, Å^3	7389.04	6105.71
ϱ_{calcd}, g cm^{-3}	1.39	1.51
μ, cm^{-1}	23.44	28.34
T, °C	22	22
λ, Å	0.710 69 (graphite monochromated, Mo Kα)	
scan type	$\omega-2\theta$	$\omega-2\theta$
2θ range, deg	5−50	5−45
scan width, deg	0.7 + 0.30 tan θ	0.7 + 0.35 tan θ
scan speed, deg min^{-1}	2.4	8.14
tot. data	14 803	6418
unique data, $I > 3\sigma$	7529	4986
no. of params	263	266
abs corr	0.88−1.17	0.84−0.99
R^a	0.054	0.048
$R_w{}^b$	0.059	0.055

$^a R = \sum||F_o| - 1/k|F_c||/\sum|F_o|$. $^b R_w = [\sum w(|F_o| - 1/k|F_c|)^2]/\sum w|F_o|^2]^{1/2}$; $\sigma(F_o) = [\sigma^2(F_o)^2 + f^2(F_o)^2]^{1/2}/2F_o$.

Preparation of $[(PP_3)Rh(\mu\text{-}H)\{Au(PPh_3)\}]PF_6$ (3a). To a THF solution (30 mL) of $[(PP_3)RhH]$ (**1**) (0.45 g, 0.58 mmol) was added a slight excess of $[Au(THF)(PPh_3)]PF_6$ prepared *in situ* from $[AuCl(PPh_3)]$ (0.30 g, 0.60 mmol) and $TlPF_6$ (0.21 g, 0.60 mmol) in THF (10 mL). Stirring the solution for 30 min produced a light orange color. Addition of ethanol (40 mL) and concentration of the resulting orange solution under nitrogen gave orange crystals of **3a**. Yield: 88%. Λ_M = 87 Ω^{-1} cm^2 mol^{-1}. Anal. Calcd for $C_{60}H_{58}AuF_6P_6Rh$: C, 52.27; H, 4.24; Rh, 7.46. Found: C, 52.06; H, 4.32; Rh, 7.30.

Preparation of $[(PP_3)Rh(\mu\text{-}H)\{Au(PPh_3)\}]BPh_4 \cdot 0.5\ C_2H_5OH$ (3b). Addition of solid $NaBPh_4$ (0.40 g, 1.17 mmol) to an acetone solution (20 mL) of **3a** (0.15 g, 0.11 mmol) gave orange crystals of the tetraphenylborate salt (**3b**) after addition of ethanol (20 mL) and slow concentration of the resulting solution under nitrogen. Yield: 92%. The crystals obtained were used for an X-ray diffraction analysis. Λ_M = 51 Ω^{-1} cm^2 mol^{-1}. Anal. Calcd for $C_{85}H_{78}AuBO_{0.5}P_5Rh$: C, 64.90; H, 5.00; Rh, 6.54. Found: C, 64.66; H, 4.93; Rh, 6.48.

Preparation of $[(NP_3)Rh(H)\{Au(PPh_3)\}]PF_6 \cdot 0.5C_4H_8O$ (4). Compound **4**, which contains NP_3 instead of PP_3, was prepared as ivory colored crystals as described above for **3a** by using **2** (0.30 g, 0.40 mmol) instead of **1**. Yield: 85%. Λ_M = 83 Ω^{-1} cm^2 mol^{-1}. IR: ν(Rh-H) 1965 cm^{-1}. Anal. Calcd for $C_{62}H_{62}AuF_6NO_{0.5}P_5Rh$: C, 53.27; H, 4.47; N, 1.00; Rh, 7.36. Found: C, 53.04; H, 4.31; N, 0.92; Rh, 7.22.

Preparation of $[(NP_3)Rh(D)\{Au(PPh_3)\}]PF_6 \cdot 0.5C_4H_8O$ (4-d_1). The monodeuterated complex **4**-d_1 was prepared as described above for **4** using **2**-d_1 and C_2H_5OD instead of **2** and C_2H_5OH.

X-Ray Diffraction Studies. A summary of crystal and intensity data for compounds **3b** and **4** is presented in Table 2. Experimental data were collected at room temperature on Philips PW1100 (**3b**) or Enraf-Nonius CAD4 (**4**) diffractometers using graphite-monochromated Mo Kα radiation. A set of 25 carefully centered reflections was used for determining the lattice constants of each crystal. As a general procedure, the intensity of three standard reflections were measured periodically every 2 h. This procedure did not reveal an appreciable decay of intensities for **3b**, whereas a slight decrease was observed for the NP_3 derivative **4**. The data were corrected for Lorentz and polarization effects. Empirical corrections for the absorption effect were performed at an advanced state of the refinements by using the program DIFABS.[15] Atomic scattering factors were those tabulated by Cromer and Waber[16] with anomalous dispersion corrections taken from ref 17. The computational work was essentially performed with the SHELX-76 system.[18] The final *R* factors are reported in Table 2.

$[(PP_3)Rh(\mu\text{-}H)\{Au(PPh_3)\}]BPh_4 \cdot 0.5C_2H_5OH$ (3b). A prismatic orange crystal with dimensions of 0.27 × 0.30 × 0.42 mm was used for the data collection. The structure was solved by using heavy-atom and Fourier techniques. Full-matrix least squares refinement were carried out with anisotropic thermal parameters only for gold, rhodium, and phosphorus atoms. The phenyl rings were treated as rigid bodies with D_{6h} symmetry with C-C bond distances fixed at 1.39 Å and calculated hydrogen atoms positions (d_{C-H} = 0.95 Å). At an advanced stage of the refinement, a molecule of solvent (ethanol) was found and refined using isotropic temperature factors and a 0.5 population parameter; all of the ethanol atoms were treated as carbon atoms. The final Fourier difference map showed clearly a peak of *ca.* 0.85 e/Å^3 near the intermetallic gold−rhodium vector in a reasonable position for a bridging hydride ligand. However, any attempt to refine the hydride positional parameters as a μ-H ligand did not lead to an acceptable convergence so that these data were not included in the model.

Final atomic coordinates and equivalent thermal factors are provided as supplementary material.

$[(NP_3)Rh(H)\{Au(PPh_3)\}]PF_6 \cdot 0.5\ C_4H_8O$ (4). A pale yellow parallelepiped crystal with dimension of 0.07 × 0.12 x 0.47 mm was used for the data collection. The structure was solved by using heavy-atom and Fourier techniques. Full-matrix least squares refinement were carried out with anisotropic thermal parameters only for Au, Rh, P, and the carbon atoms of the NP_3 backbone. The phenyl rings were treated as rigid bodies with D_{6h} symmetry with C-C bond distances fixed at 1.39 Å and the hydrogen atoms were introduced in calculated positions (d_{C-H} = 0.95 Å). The final difference maps revealed the presence of a disordered molecule of tetrahydrofuran which was attributed a population factor of 0.5. In no case were attempts to assign the O atom position in the five-membered ring of the solvent model made and, consequently, all of the solvent atoms were treated as carbon atoms. Upon convergence, the Fourier difference map showed a peak (approximately 0.7 e/Å^3) at R = 0.058. This was found in an acceptable position for a terminal hydride ligand and, hence, retained and succesfully refined as a hydride ligand, although the esd's were high, as expected, using an isotropic temperature factor.

Final atomic coordinates and equivalent thermal factors are provided as supplementary material.

Results and Discussion

Synthesis of the Rhodium−Gold Hydrides. The addition of 1 equiv of $[Au(THF)(PPh_3)]PF_6$, prepared *in situ* by treatment of $[AuCl(PPh_3)]$ with $TlPF_6$, to THF solutions of the trigonal-bipyramidal Rh(I) monohydrides $[(PP_3)RhH]$ (**1**) or $[(NP_3)RhH]$ (**2**) under nitrogen results in almost quantitative formation of orange or ivory crystals of $[(PP_3)Rh(\mu\text{-}H)\{Au(PPh_3)\}]PF_6$ (**3a**) and $[(NP_3)Rh(H)\{Au(PPh_3)\}]PF_6 \cdot 0.5C_4H_8O$ (**4**), respectively. Metathetical reaction of **3a** with $NaBPh_4$ in acetone/ethanol affords the tetraphenylborate salt $[(PP_3)Rh(\mu\text{-}H)\{Au(PPh_3)\}]BPh_4 \cdot 0.5C_2H_5OH$ (**3b**) (Scheme 1).

X-ray Diffraction Studies. Single-crystal X-ray diffraction analyses have been carried out on **3b** and **4**. A list of selected bond lengths and angles for both compounds is provided in Table 3, while ORTEP[19] views of the complex cations $[(PP_3)Rh(\mu\text{-}H)\{Au(PPh_3)\}]^+$ and $[(NP_3)Rh(H)\{Au(PPh_3)\}]^+$ are shown in Figures 1 and 2, respectively.

$[(PP_3)Rh(\mu\text{-}H)\{Au(PPh_3)\}]BPh_4 \cdot 0.5C_2H_5OH$. The crystal structure of **3b** consists of discrete $[(PP_3)Rh(\mu\text{-}H)\{Au(PPh_3)\}]^+$

(15) Walker, N.; Stuart, D. *Acta Crystallogr.* **1983**, *A39*, 158.

(16) Cromer, D. T.; Waber, J. T. *Acta Crystallogr.* **1965**, *18*, 104.

(17) *International Tables of Crystallography*; Kynoch Press: Birmingham, U.K., 1974.

(18) Sheldrick, G. M. *SHELX-76. A program for crystal structure determination*; University of Cambridge: Cambridge, U.K., 1976.

(19) Johnson, C. K. Report *ORNL-5138*; Oak Ridge National Laboratory: Oak Ridge, TN, 1976.

Scheme 1

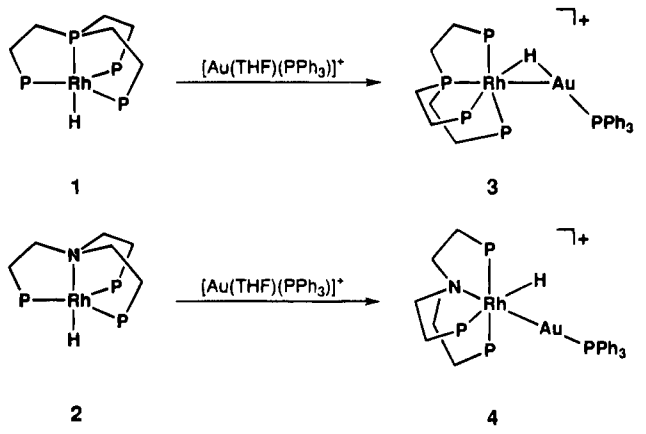

Table 3. Selected Bond Lengths (Å) and Angles (deg) for the Complexes $[(PP_3)Rh(\mu\text{-}H)\{Au(PPh_3)\}]BPh_4{\cdot}0.5C_2H_5OH$ (**3b**) and $[(NP_3)Rh(H)\{Au(PPh_3)\}]PF_6{\cdot}0.5C_4H_8O$ (**4**)

	3b	4		3b	4
Au–Rh	2.690(1)	2.531(1)	Rh–Au–P(4)		176.3(1)
Au–P(4)		2.281(3)	Au–Rh–H		93(4)
Au–P(5)	2.267(3)		Rh–Au–P(5)	169.3(1)	
Rh–P(1)	2.302(3)	2.257(3)	Au–Rh–N		175.9(3)
Rh–P(2)	2.293(3)	2.268(3)	Au–Rh–P(1)	88.9(1)	97.9(1)
Rh–P(3)	2.232(3)	2.316(3)	Au–Rh–P(2)	116.6(1)	91.0(1)
Rh–P(4)	2.219(37		Au–Rh–P(3)	82.6(1)	92.9(1)
Rh–N		2.27(1)	Au–Rh–P(4)	157.2(1)	
Rh–H		1.55(9)	P(1)–Rh–P(2)	119.6(1)	147.8(1)
P(1)–C(1)	1.85(1)	1.85(1)	P(1)–Rh–P(3)	127.0(1)	104.3(1)
P(2)–C(3)	1.83(1)	1.88(1)	P(1)–Rh–P(4)	84.6(1)	
P(3)–C(5)	1.84(1)	1.86(2)	P(2)–Rh–P(3)	110.8(1)	106.1(1)
P(4)–C(2)	1.82(1)		P(2)–Rh–P(4)	85.3(1)	
P(4)–C(4)	1.84(1)		P(3)–Rh–P(4)	83.9(1)	
P(4)–C(6)	1.82(1)		N–Rh–H		89(4)
N–C(2)		1.50(2)	P(1)–Rh–H		76(4)
N–C(4)		1.51(2)	P(2)–Rh–H		73(4)
N–C(6)		1.49(2)	P(3)–Rh–H		173(4)
C(1)–C(2)	1.51(2)	1.48(2)	P(1)–Rh–N		85.9(3)
C(3)–C(4)	1.49(2)	1.51(2)	P(2)–Rh–N		86.6(3)
C(5)–C(6)	1.55(2)	1.52(2)	P(3)–Rh–N		84.6(3)

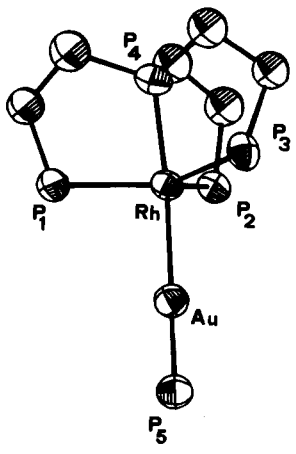

Figure 1. ORTEP drawing of the complex cation $[(PP_3)Rh(\mu\text{-}H)\{Au(PPh_3)\}]^+$ in **3b**. All of the phenyl rings and hydrogen atoms have been omitted for clarity.

cations, PF_6^- anions, and clathrated ethanol molecules in a ratio of 1:1:0.5 with no unusual intramolecular contacts.

The geometry of the coordination polyhedron around rhodium approximates a trigonal bipyramid. The three peripheral P atoms of the polyphosphine ligand occupy the three equatorial positions of the coordination polyhedron, while the bridgehead phosphorus atom and the gold–phosphine fragment are located *transoid* to each other in axial positions. The three equatorial angles range from 110.8(1) to 127.0(1)° and, therefore, do not markedly differ from the values expected for a trigonal-bipyramidal complex. The rhodium atom lies 0.22 Å away from the plane defined by the equatorial phosphorus atoms, toward the gold atom. Similar displacements of the metal center from the equatorial plane are currently observed in trigonal-bipyramidal rhodium compounds containing the PP_3 ligand (range 0.22–0.27 Å).[20]

Even though the hydride ligand bridging the $(PP_3)Rh$ and $Au(PPh_3)$ moieties was not safely determined in the course of the X-ray analysis, its presence is unambiguously shown by a combination of both spectroscopic and structural data. In particular, in order to fulfil the stereoelectronic requirements of the μ-H ligand, the Rh–Au vector is significatively tilted from the normal to the plane containing the rhodium and the equatorial P donors of PP_3; the three-atom sequences P(4)–Rh–Au and Rh–Au–P(5) are not linear [angles 157.2(1) and 169.3(1)°, respectively] with apparent bending of the Rh–Au–(PPh_3) moiety toward the cradle of the slightly opened P(1)–Rh–P(3) angle [127.0(1)°]. In keeping with this deformation, the Au–Rh–P_{eq} angles are far from being equivalent: two of them are acute [Au–Rh–P(1), 88.9(1)°; Au–Rh–P(3), 82.6(1)°] while the third is obtuse [Au–Rh–P(2), 116.9(1)°]. Similar angular distortions of the non-hydrogen skeleton of the molecule have previously been reported for a series of heteronuclear hydrido-bridged bimetallic compounds containing coinage metals and have been ascribed to the presence of a stereochemically active bridging hydride ligand.[21–23] In some cases, the μ-hydride ligands have unambiguously been localized by X-ray methods;[24–27] in most instances, however, the bonding mode of the μ-hydride has been established only from indirect structural data, NMR spectroscopy, or potential energy calculations.[21–23,28–34] In the present case, the presence of a bridging hydride ligand is confirmed, beyond any reasonable

(20) (a) Di Vaira, M.; Peruzzini, M.; Stoppioni, P. *Inorg. Chem.* **1991**, *30*, 1001. (b) Di Vaira, M.; Peruzzini, M.; Stoppioni, P. *Inorg. Chem.* **1989**, *28*, 4614. (c) Di Vaira, M.; Rovai, D.; Stoppioni, P. *Polyhedron* **1993**, *12*, 13.
(21) Mueting, A. M.; Bos, W.; Alexander, B. D.; Boyle, P. D.; Casalnuovo, J. A.; Balaban, S.; Ito, L. N.; Johnson, S. M.; Pignolet, L. H. *New J. Chem.* **1988**, *12*, 505.
(22) Salter, I. D. *Adv. Organomet. Chem.* **1989**, *29*, 249.
(23) Mingos, D. M. P.; Watson, M. J. *Adv. Inorg. Chem.* **1992**, *39*, 237.
(24) (a) Albinati, A.; Lehner, H.; Venanzi, L. M.; Wolfer, M. *Inorg. Chem.* **1987**, *26*, 3933. (b) Albinati, A.; Anklin, C.; Janser, P.; Lehner, H.; Matt, D.; Pregosin, P. S.; Venanzi, L. M. *Inorg. Chem.* **1989**, *28*, 1105. (c) Albinati, A.; Venanzi, L. M.; Wang, G. *Inorg. Chem.* **1993**, *32*, 3660. (d) Albinati, A.; Eckert, J.; Hofmann, P.; Rüegger, H.; Venanzi, L. M. *Inorg. Chem.* **1993**, *32*, 2277.
(25) Green, M.; Orpen, A. G.; Salter, I. D.; Stone, F. G. A. *J. Chem. Soc., Dalton Trans.* **1984**, 2497.
(26) (a) Alexander, B. D.; Gomez-Sal, M. P.; Gannon, P. R.; Blaine, C. A.; Boyle, P. D.; Mueting, A. M.; Pignolet, L. H. *Inorg. Chem.* **1988**, *27*, 3301. (b) Alexander, B. D.; Johnson, B. J.; Johnson, S. M.; Boyle, P. D.; Kann, N. C.; Mueting, A. M.; Pignolet, L. H. *Inorg. Chem.* **1987**, *26*, 3506. (c) Alexander, B. D.; Johnson, B. J.; Johnson, S. M.; Casalnuovo, A. L.; Pignolet, L. H. *J. Am. Chem. Soc.* **1986**, *108*, 4409.
(27) Bianchini, C.; Meli, A.; Peruzzini, M.; Vacca, A.; Vizza, F.; Albinati, A. *Inorg. Chem.* **1992**, *31*, 3841.
(28) Antiñolo, A.; Jalon, F. A.; Otero, A.; Fajardo, M.; Chaudret, B.; Lahoz, F.; López, J. A. *J. Chem. Soc., Dalton Trans.* **1991**, 1861.
(29) Crespo, M.; Sales, J.; Solans, X. *J. Chem. Soc., Dalton Trans.* **1989**, 1089.
(30) Boyle, P. D.; Johnson, B. J.; Alexander, B. D.; Casalnuovo, J. A.; Gannon, P. R.; Johnson, S. M.; Larka, E. A.; Mueting, A. M.; Pignolet, L. H. *Inorg. Chem.* **1987**, *26*, 1346.
(31) Socol, S. M.; Meek, D. W.; Glaser, R. *Polyhedron* **1989**, *8*, 1903.
(32) Orpen, A. G. *J. Chem. Soc., Dalton Trans.* **1980**, 2509.
(33) Henrick, K.; McPartlin, M.; Morris, J. *Angew. Chem., Int. Ed. Engl.* **1986**, *25*, 853.
(34) Alexander, B. D.; Mueting, A. M.; Pignolet, L. H. *Inorg. Chem.* **1990**, *29*, 1313.

Table 4. Comparison of Selected Structural Parameters for Bimetallic Transition-Metal Gold–Phosphine Adducts

	M–Au (Å)	Au–P (Å)	M–P_{av} (Å)	M–Au–P (deg)	ref
	Terminal Au(PR_3) Fragments				
1, $[(dppe)_2Ir\{Au(PPh_3)\}]^{2+}$ [a]	2.651(1)	2.219(5)	2.357(5)	168.7(1)	62
2, $[IrH(CO)(PPh_3)_3\{Au(PPh_3)\}]^{+}$ [e]	2.662(1)	2.293(2)	2.367(2)	165.53(7)	63
3, $[Pt_3(\mu_3\text{-}S)\{Au(PPh_3)\}(\mu_3\text{-}AgCl)(\mu\text{-}dppm)_3]^{+}$ [b,d]	2.576(3)	2.276(11)	2.275(11)	174.2(3)	64
4, $[(NP_3)Rh(H)\{Au(PPh_3)\}]^{+}$ [e]	2.531(1)	2.281(3)	2.280(3)	176.3(1)	this work
	Hydride-Bridged Au(PR_3) Fragments				
5, $[Ir(PPh_3)_3(H)_2(\mu\text{-}H)\{Au(PPh_3)\}]^{+}$ [f]	2.765(1)	2.265(5)	2.352(6)	155.3(3)	24b
6, $[Ir(bpy)(PPh_3)_2(\mu\text{-}H)_2\{Au(PPh_3)\}]^{2+}$ [c,d]	2.699(1)	2.239(2)		168.6(1)	26c
7, $[Pt(C_6F_5)(PEt_3)_2(\mu\text{-}H)\{Au(PPh_3)\}]^{+}$ [e]	2.714(1)	2.264(4)	2.315(4)	146.38(1)	24a
8, $[Pt(C_6Cl_5)(PPh_3)_2(\mu\text{-}H)\{Au(PPh_3)\}]^{+}$ [d]	2.792(1)	2.293(8)	2.323(4)	160.9(2)	29
9, $[(CO)_5Cr(\mu\text{-}H)\{Au(PPh_3)\}]$ [e]	2.770(2)	2.290(3)		155.4(1)	25
10, $[Ru(dppm)_2(\mu\text{-}H)_2\{Au(PPh_3)\}]^{+}$ [e]	2.694(1)	2.252(2)	2.331(2)	170.95(5)	26b
11, $[Ru(PPh_3)_3(CO)(\mu\text{-}H)_2\{Au(PPh_3)\}]^{+}$ [e]	2.786(1)	2.279(2)	2.411(2)	163.50(5)	26a
12, $[(PP_3)Rh(\mu\text{-}H)\{Au(PPh_3)\}]^{+}$ [d]	2.690(1)	2.267(3)	2.261(3)	169.3(1)	this work

[a] dppe = $Ph_2PCH_2CH_2PPh_2$. [b] dppm = $Ph_2PCH_2PPh_2$. [c] bpy = bypyridine. [d] The hydride ligand was not located by X-ray methods. [e] The hydride ligand was located by X-ray methods. [f] The hydride ligand was located trough computational methods (HYDEX program; see ref 32).

doubt, by multinuclear NMR spectroscopy as well as a number of geometrical features affecting the $(PP_3)RhAu(PPh_3)$ assembly.

The Rh-Au distance in **3b** [2.690(1) Å] is significatively longer than the sum of the covalent radii for the two metals (*ca.* 2.59 Å) and longer than the analogous distance in the related complex **4** [2.531(1) Å] which contains a terminal hydride ligand (*vide infra*). Moreover, the RhAu separation in **3b** matches well the values observed in higher nuclearity rhodium-gold clusters containing μ-H ligands.[34] As an example, the average RhAu bond length in the compound of Venanzi *et al.* [(triphos)Rh-(μ-H)$_2${Au(PPh_3)}$_3$]$^{2+}$ is 2.695(2) Å [triphos = $MeC(CH_2PPh_2)_3$],[35] whereas in the complex cation $[(PPh_3)_2(CO)Rh(\mu\text{-}H)\{Au(PPh_3)\}_3]^{+}$ described by Pignolet and co-workers, the RhAu separations of the three unequivalent rhodium–gold bonds range from 2.640(3) to 2.722(3) Å.[36] In the latter complex, the presence of a hydride ligand asimmetrically bridging one edge of the $RhAu_3$ tetrahedron was confirmed by an X-ray analysis.

The Au-P [2.267(3) Å] and Rh-P [2.261(3)$_{av}$ Å] bond lengths in **3b** are comparable with those of several phosphine complexes of gold[37,38] and rhodium,[20,37] respectively, and, thus, do not deserve additional comments. In contrast, it is worth mentioning that the Rh-P(3) bond *trans* to the bridging hydride [2.232(3) Å] is even shorter than the analogous distances pertaining to the two mutually *trans* phosphorus atoms P(1) and P(2) [2.302-(3) and 2.293(3) Å, respectively]. This finding is in agreement with previous observations according to which μ-H ligands exert a much weaker *trans* influence than terminal hydrides.[26c,39,40]

Due to the small number of transition metal–gold hydrides authenticated by X-ray diffraction analysis, it is not possible to provide a general structural trend for distinguishing the bonding mode of the hydride in these compounds. However, from a perusal of Table 4, which compares relevant structural parameters of metal–gold complexes containing either terminal or μ-H supported gold–phosphine fragments, one may infer that the compounds with an M(μ-H)Au bonding mode exhibit longer M–Au separations than unsupported M–Au compounds. In keeping with this observation, the Rh–Au distance in **3b** is significantly longer than in **4** [Δd_{Rh-Au} = 0.159(1) Å]. A similar structural relationship has previously been proposed for homonuclear bimetallic complexes containing either M-(μ-H)M or M–M assemblies.[41]

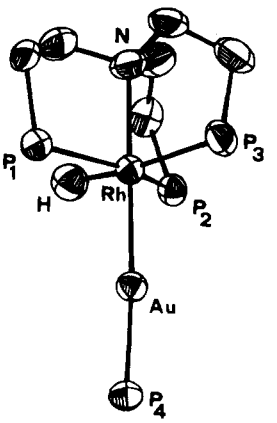

Figure 2. ORTEP drawing of the complex cation $[(NP_3)Rh(H)\{Au(PPh_3)\}]^{+}$ in **4**. All of the phenyl rings and, except for the terminal hydride ligand, hydrogen atoms have been omitted for clarity.

$[(NP_3)Rh(H)\{Au(PPh_3)\}]PF_6 \cdot 0.5C_4H_8O$. The crystal structure of **4** consists of discrete mononuclear $[(NP_3)Rh(H)\{Au(PPh_3)\}]^{+}$ cations, tetraphenylborate anions, and clathrated tetrahydrofuran molecules in a stoichiometric ratio of 1:1:0.5.

The rhodium atom is coordinated in a distorted octahedral geometry by the nitrogen and the three phosphorus atoms of NP_3 ligand, by the gold atom from the $[Au(PPh_3)]$ fragment, *trans* to nitrogen, and by a hydride ligand which does not show any intramolecular bonding contact to gold [$d_{Au\cdots H}$ = 3.04 Å]. As expected, the hydride ligand exerts the highest *trans* influence, the Rh–P(3) bond length [2.316(3) Å] being the longest of the three Rh–P separations [Rh–P(1) 2.257(3) Å, Rh–P(2) 2.268(3) Å]. The Rh–N [2.27(1) Å] and the three Rh–P bond distances are in good correlation with those of several octahedral complexes containing the $(NP_3)M$ moiety.[3eh,5b,20b,42] Indeed, the arrangement of the NP_3 ligand about the metal in **4** does not fully conform to the butterfly shaped which is proper of L_4M fragments with C_{2v} symmetry. This is clearly shown by the two mutually *trans* PPh_2 groups which are significatively bent over the plane defined by Rh, H, and Au with the angle

(35) Albinati, A.; Demartin, F.; Janser, P.; Rhodes, L. F.; Venanzi, L. M. *J. Am. Chem. Soc.* **1989**, *111*, 2115.
(36) Boyle, P. D.; Johnson, B. J.; Buchler, A.; Pignolet, L. H. *Inorg. Chem.* **1986**, *25*, 5.
(37) Orpen, A. G.; Brammer, L.; Allen, F. H.; Kennard, O.; Watson, D. G.; Taylor, R. *J. Chem. Soc., Dalton Trans.* **1989**, S1.
(38) Puddephatt, R. J. In *Comprehensive Coordination Chemistry*; Wilkinson, G., Ed.; Pergamon Press: New York 1987; Vol. V, pp 861–923.
(39) Alexander, B. D.; Johnson, B. J.; Boyle, P. D.; Kann, N. C.; Mueting, A. M.; Pignolet, L. H. *Inorg. Chem.* **1987**, *26*, 3503.
(40) Immirzi, B. D.; Porzio, W.; Bachechi, F.; Zambonelli, L.; Venanzi, L. M. *Gazz. Chim. Ital.* **1983**, *113*, 537.
(41) (a) Teller, R. G.; Bau, R. *Struct. Bonding (Berlin)* **1981**, *44*, 1. (b) Bau, R.; Teller, R. G.; Kirtley, S. W.; Koetzle, T. F. *Acc. Chem. Res.* **1979**, *12*, 176.
(42) Di Vaira, M.; Peruzzini, M.; Stoppioni, P.; Zanobini, F. *Inorg. Chim. Acta* **1983**, *69*, 37.

P(1)−Rh−P(2) equal to 147.8(1)°. Analogous deformations have been observed in other octahedral metal complexes with the NP_3 and PP_3 ligands.[2−6,20,42,43]

The N−Rh−Au and Au−Rh−P(5) arrays are almost linear [175.9(1) and 176.3(1)°, respectively]. Moreover, the Rh−H separation [1.55(1) Å] matches well the values found in several rhodium complexes with terminal hydride ligands.[3e,44] Finally, the present Rh−Au bond distance [2.531(1) Å] is the shortest ever reported for complexes containing either supported or unsupported Rh−Au bonds [range: 2.640−3.147 Å].[21,23,34,36,44−51] In particular, it is shorter than that found in the cognate compound **3b** [2.690(1) Å] which contains a μ-H ligand.

Spectroscopic Properties of the Rhodium−Gold Monohydrides. As a consequence of the different bonding mode of the hydride ligand, the rhodium−gold hydrides **3a,b** and **4** significantly differ in their spectroscopic properties. In particular, the IR spectrum of **4** exhibits a medium intensity band at *ca.* 1965 cm^{-1} which diagnoses the presence of a terminal hydride ligand.[3,5,20a] This absorption disappears in the IR spectrum of the monodeuterated complex $[(NP_3)Rh(D)\{Au(PPh_3)\}]PF_6$ (**4**-d_1). However, no band in the IR spectrum of the d_1-isotopomer could confidently be associated with ν(Rh−D) because of overlapping of isoenergetic absorptions due to the polyphosphine ligand in the range expected for Rh−D stretching modes [1400−1450 cm^{-1} for a $k_{H/D}$ value of 1.35−1.40].[52]

The IR spectra of the PP_3 derivatives **3a,b** do not show any absorption ascribable to bridging hydrides [ν(Rh−H−Au) modes]. Indeed, these vibrations are generally very weak and thus difficult to detect in metal−gold clusters containing μ-H ligands.[21,23]

$^{31}P\{^1H\}$ NMR Spectra. Since the counteranion does not influence at all the NMR properties of **3a,b**, the relevant data reported in Table 1 refer to the complex cation $[(PP_3)Rh(\mu\text{-}H)\{Au(PPh_3)\}]^+$, hereafter quoted as **3**.

Complex **3** is stereochemically nonrigid on the NMR time scale in the temperature range from +30 to −100 °C. The room temperature spectrum in CD_2Cl_2 consists of a first-order AM_3QX splitting pattern indicating the equivalence of the three terminal phosphorus atoms of PP_3. This spin system is diagnostic for a trigonal-bipyramidal environment around the metal center in PP_3 complexes.[2−5,20,43] In the case at hand, each resonance is perturbed by additional couplings to the gold−phosphine P atom (P_Q), which resonates in the expected low-field region of the spectrum, and to the NMR active ^{103}Rh nucleus (X). The chemical shifts and coupling constants pertaining to the AM_3 part of the spectrum nicely correlate with those reported for a plethora of trigonal bipyramidal $(PP_3)Rh(I)$ complexes.[3,5,20,53] In particular, the Rh−P coupling constants [$J(P_ARh)$ 104.6 Hz, $J(P_MRh)$ 136.3 Hz] are larger than those found for Rh(III) complexes (<100 Hz). The bridgehead phosphorus atom of the PP_3 ligand shows a three-bond coupling to the gold−phosphine atom of 46.7 Hz. This value is much smaller than that found for the trigonal-bipyramidal Pt complex $[(PP_3)Pt\{Au(PPh_3)\}]BPh_4$ for which a $^3J(P_{ap}P_{Au})$ value of 164 Hz is reported.[54] Accordingly, the reduced $J(P_AP_Q)$ value in **3** is strongly indicative of an active stereochemical role played by the μ-H ligand, which is consistent with the solid-state structure.

On decreasing the temperature, down to as much as −100 °C, the chemical shifts of the three phosphorus nuclei do not appreciably change. Only a slight broadening of all signals occurs, indicating that at this point the slow-exchange spectrum has not been reached.

Similar variable-temperature $^{31}P\{^1H\}$ NMR spectra (CD_2Cl_2) are shown by the NP_3 derivative **4**. At room temperature, the spectrum consists of two doublets in line with an A_3MX splitting pattern with $J(P_AP_M) = 0$. Interestingly, the two-bond *Rh*-Au-*P* coupling constant [$J(P_MRh)$ 11.7 Hz] in **4** is slightly larger than in the PP_3 derivatives **3** [$J(P_QRh)$ 8.7 Hz]. These finding is in line with a previous observation by Peringer *et al.* for the Pt complexes $[(PP_3)Pt\{Au(PPh_3)\}]BPh_4$ and $[(NP_3)Pt\{Au(PPh_3)\}]BPh_4$ and reflects the different *trans* influence exerted by nitrogen and phosphorus donors.[54]

The stereochemical nonrigidity which equilibrates the three phosphorus atoms of NP_3 remains operative also at the lowest temperature investigated (−100 °C). Indeed, as the temperature is decreased, we observe only loss of resolution in low-field resonance which at −100 °C appears as a broad hump with $w_{1/2}$ = 335 Hz.

^1H NMR Spectra. Valuable information for elucidating the solution structure of **3** and **4** and, thus, for unambiguously establishing that the different bonding mode of the hydride ligand observed in the solid-state persists in solution is provided by a comparison of the ^1H NMR spectra of **3** and **4** in the hydride region (Figures 3 and 4).

In particular, the ^1H NMR spectrum of **3** (CD_2Cl_2, 21 °C) contains a resonance at δ −3.74 in the form of a well-resolved AM_3QXY (Y = $H_{hydride}$) spin system. The 32-line pattern appears as eight binomial quartets separated by three inequivalent splittings. The quartets [$^2J(HP_M)$ 3.9 Hz] witness the magnetic equivalence of the three exchanging terminal phosphorus atoms. Broad-band decoupling and selective irradiation of the phosphorus resonances allow one to evaluate the magnitude of the geminal $^2J(HP)$ coupling constants [$^2J(HP_A)$ 84.3 Hz, $^2J(HP_Q)$ 50.9 Hz] and of the one-bond coupling to the rhodium atom [$^1J(HRh)$ 17.8 Hz]. Some of these coupling connections contribute to the understanding of the molecular structure in solution. In particular, the magnitude of the heteronuclear coupling constant [50.9 Hz] is consistent with the presence of a μ-H ligand. In fact, as reported by Pignolet and co-workers,[21] M-(μ-*H*)−Au−*P* couplings > 20 Hz are diagnostic of bridging hydrides, whereas values < 15 Hz are indicative of *H*−M−Au−*P* sequences with no H−Au bonding

(43) (a) Bianchini, C.; Pèrez, P. J.; Peruzzini, M.; Zanobini, F.; Vacca, A. *Inorg. Chem.* **1991**, *30*, 279. (b) Bianchini, C.; Peruzzini, M.; Zanobini, F.. Frediani, P.; Albinati, A. *J. Am. Chem. Soc.* **1991**, *113*, 5543. (c) Bianchini, C.; Masi, D.; Linn, K.; Mealli, C.; Peruzzini, M.; Zanobini, F. *Inorg. Chem.* **1992**, *31*, 4036. (d) Bianchini, C.; Linn, K.; Masi, D.; Peruzzini, M.; Polo, A.; Vacca, A.; Zanobini, F. *Inorg. Chem.* **1993**, *32*, 2366 (e) Wolinska, A.; Touchard, D.; Dixneuf, P. H. Romero, A. *J. Organomet. Chem.* **1991**, *420*, 217.
(44) Fernández, M.-J.; Bailey, P. M.; Bentz, P. O.; Ricci, J. S.; Koetzle, T. F.; Maitlis, P. M. *J. Am. Chem. Soc.* **1984**, *106*, 5458.
(45) Pursianen, J.; Åhlgrén, M.; Pakkanen, T. A. *J. Organomet. Chem.* **1985**, *297*, 391.
(46) Fernández, M.-J.; Modrego, J.; Oro, L. A.; Apreda, M.-C.; Cano, F. H.; Foces-Foces, C. *J. Chem. Soc., Dalton Trans.* **1989**, 1249.
(47) Fumagalli, A.; Martinengo, S.; Albano, V. G.; Braga, D. *J. Chem. Soc., Dalton Trans.* **1988**, 1237.
(48) Fumagalli, A.; Martinengo, S.; Albano, V. G.; Braga, D.; Grepioni, F. *J. Chem. Soc., Dalton Trans.* **1989**, 2343.
(49) Schiavo, S. L.; Bruno, G.; Nicolò, F.; Piraino, P.; Faraone, F. *Organometallics* **1985**, *4*, 2091.
(50) Carr, N.; Gimeno, M. G.; Goldberg, J. E.; Pilotti, M. U.; Stone, F. G. A.; Topaloglu, I. *J. Chem. Soc., Dalton Trans.* **1990**, 2553.
(51) Jeffery, J. C.; Jelliss, P. A.; Stone, F. G. A. *J. Chem. Soc., Dalton Trans.* **1993**, 1073.
(52) See for example: Ebsworth, E. A. V.; Rankin, D. W. H.; Cradock, S. *Structural methods in inorganic chemistry*, 2nd ed.; Blackwell Sci. Publ.: Oxford, U.K., 1991; Chapter V.
(53) Gambaro, J. J.; Hohman, W. H.; Meek, D. W. *Inorg. Chem.* **1989**, *28*, 4154.
(54) Peter, M.; Peringer, P.; Müller, E. P. *J. Chem. Soc., Dalton Trans.* **1991**, 2459.

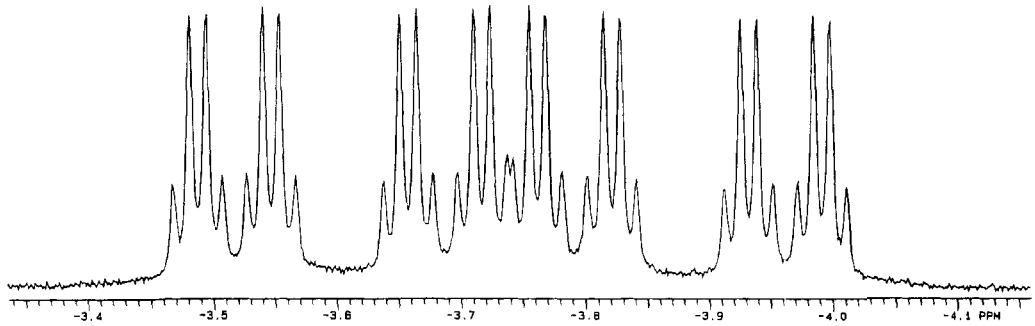

Figure 3. ^{1}H NMR resonance of the hydride ligand in $[(PP_3)Rh(\mu\text{-}H)\{Au(PPh_3)\}]^+$ (CD_2Cl_2, 21 °C, 299.94 MHz, TMS reference).

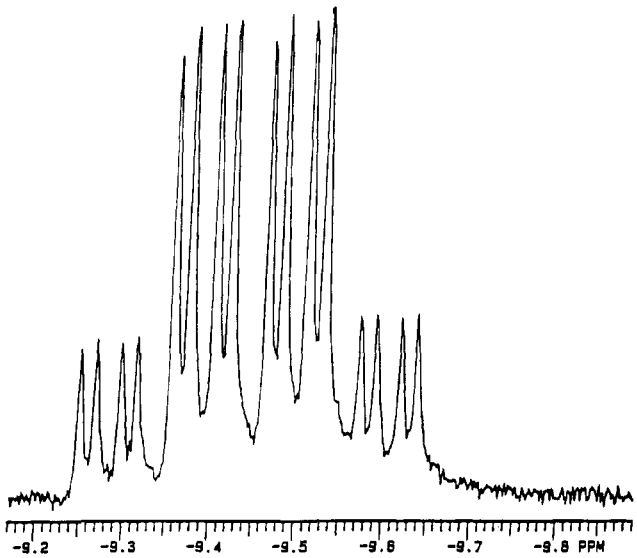

Figure 4. ^{1}H NMR resonance of the hydride ligand in $[(NP_3)Rh(H)\{Au(PPh_3)\}]^+$ (CD_2Cl_2, 21 °C, 299.94 MHz, TMS reference).

interaction. Consistently, values higher than 40 Hz have recently been reported for the iridium complexes [(triphos)Ir(H)(C_2H_4){Au(PPh_3)}]PF_6 and [(triphos)Ir(Cl)(H){$Au_2(PPh_3)_2$}]PF_6 where the presence of a bridging hydride ligand has unambiguously been established.[27] Also, the reduced magnitude of $J(HP_{Au})$ in gold clusters with μ-H ligands has been associated with the occurrence of dynamic processes averaging the spin–spin couplings to lower values than those observed for rigid *trans* stereochemistries.[21]

The large value of $^2J(HP_A)$ in **3** points to a strong coupling between these two nuclei. The $^2J(HP_A)$ value, although smaller than that measured for the parent monohydride **1** [$^2J(HP_{trans})$ 130.0 Hz],[5] is significatively larger than those pertaining to $^2J(HP_{cis})$ couplings generally observed in $(PP_3)Rh$ hydrido complexes (9–18 Hz).[3,5,20a]

Finally, it is worth mentioning that the chemical shift of the hydride ligand in **3** is significantly shifted downfield as compared to **4** as well as other $(PP_3)Rh$ complexes with terminal hydride ligands [−8 to −10 ppm].[3,5a,20a] The T_1 value exhibited by **3** (740 ± 20 ms in acetone-d_6, 20 °C, 300 MHz, inversion–recovery sequence) is shorter than that measured for the monohydride **1** under identical experimental conditions (1160 ± 20 ms). The shorter T_1 value of the gold adduct is reasonably due to the gold–hydride interaction which is expected to contribute to the dipolar relaxation mechanism.[27,55]

In keeping with the structural data, the NP_3 derivative **4** exhibits a hydride resonance at higher field (δ_H −9.44, A_3MXY pattern, Y = $H_{hydride}$), which diagnoses the presence of a terminal H ligand. The signal appears as a quartet of doubled doublets (Figure 4). Selective heteronuclear decoupling experiments provide the coupling constants pertaining to the hydride ligand. Of particular relevance, is the three-bond coupling $J(HP_M)$ of only 5.6 Hz, which indicates the absence of bonding interaction of the hydride ligand with the gold atom.[21]

Variable-temperature ^{1}H NMR studies on **3** or **4** are uninformative since the dynamic processes affecting both compounds are only slowed down at low temperature. Broadening of the hydride resonances occurs, but the slow exchange regime was not attained even at −100 °C.

^{103}Rh NMR Spectra. The ^{103}Rh NMR data of compounds **1**–**4** have been compiled in Table 1 and have been acquired *via* inverse ^{1}H,{^{103}Rh} NMR spectroscopy, which is the method of choice when, as in the present cases, $J(HRh)^{-1}$ is small compared to T_2 of the hydride nuclei. The ^{1}H,{^{103}Rh} spectra of compounds **3** and **4** are shown in Figures 5 and 6, respectively. The Rh chemical shift has been interpolated from the F_1 trace of the 2D spectrum with an accuracy of ±1 ppm, which is determined by the digital resolution in F_1. Due to the 180° proton pulse in the middle of the evolution period, proton coupling is removed (as only one hydride is present) from the ^{103}Rh domain. As the spin states of the ^{31}P nuclei are not being affected during the pulse sequence, the ^{103}Rh resonance line is split by scalar coupling due to phosphorus nuclei and hence appears as a quartet (**2**), a doublet of quartets (**1**), a quartet of doublets (**4**), and a quartet of doublets of doublets (**3**) in ^{103}Rh domain.

From the spectra not only the ^{1}H and ^{103}Rh chemical shifts but also the coupling constants $^2J(HRh)$, $^nJ(HP)$, and $^1J(PRh)$ including their (relative) sign can be deduced directly. *E.g.* for **3**, the Rh peaks at low frequency in F_1 correlate with the high-frequency hydride signals in the multiplet associated with $^2J(HP_Q)$ coupling along F_2, whereas for $^2J(HP_A)$ and $^1J(HRh)$ the opposite is observed. As the latter will be negative (Rh has a negative gyromagnetic ratio), $^2J(HP_A)$ is also negative and $^2J(HP_M)$ and $^2J(HP_Q)$ are positive. Similar assignments can be made for $J(PRh)$ in **3**; where $^1J(P_MRh)$ is of opposite sign relative to both $^1J(P_ARh)$ and $^2J(P_QRh)$.

Similarly, one finds for **4** that the $^1J(P_ARh)$ and $^2J(P_MRh)$ are of opposite sign compared to $^1J(P_MRh)$ and $^2J(P_QRh)$, respectively, in **3**. For the $^2J(HP_A)$ and $^2J(HP_M)$ in **4**, which compare with $^2J(HP_M)$ and $^2J(HP_Q)$ in **3**, it is seen that, taking $^1J(HRh)$ as negative again, $^2J(HP_M)$ is positive, whereas $^2J(HP_A)$ is negative, i.e. the opposite as observed in **3**.

Apparently, the $^2J(HP_{eq})$ is of opposite sign in these complexes. Similarly, $^3J(HP_{Au})$ is of opposite sign, and within **3** $^2J(HP_{ap})$ is of the same sign as $^3J(HP_{Au})$. All these data point to dissimilar structures for **3** and **4** as far as the coordination of the hydride is concerned, an observation which is also clearly reflected by the large difference in the ^{103}Rh chemical shift for these complexes (*vide infra*).

(55) (a) Gusev, D. G.; Vymenits, A. B.; Bakhmutov, V. I. *Inorg. Chem.* **1991**, *30*, 3118. (b) Desrosiers, P.; Cai, L.; Lin, Z.; Richards, R.; Halpern, J. *J. Am. Chem. Soc.* **1991**, *113*, 4173.

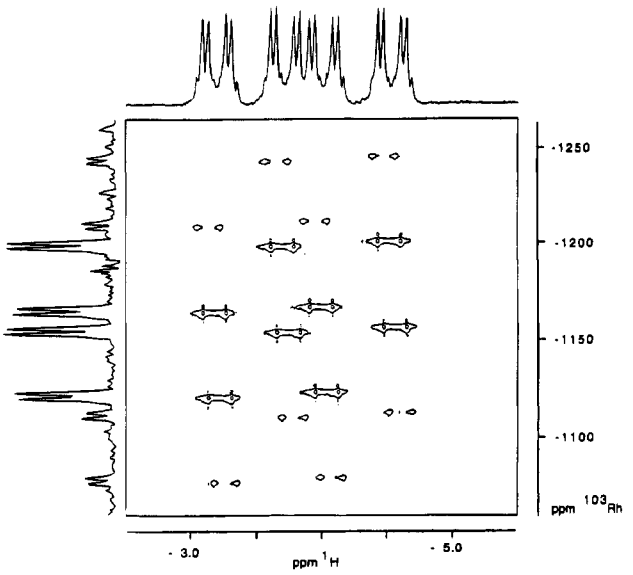

Figure 5. Contour plot of an inverse $^1H,\{^{103}Rh\}$ NMR spectrum of $[(PP_3)Rh(\mu\text{-}H)\{Au(PPh_3)\}]^+$ (CD_2Cl_2, 30 °C, 100.13 MHz).

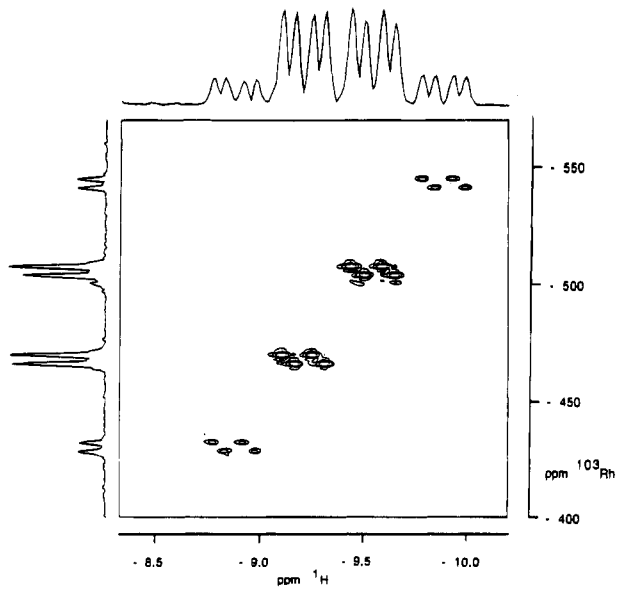

Figure 6. Contour plot of an inverse $^1H,\{^{103}Rh\}$ NMR spectrum of $[(NP_3)Rh(H)\{Au(PPh_3)\}]^+$ (acetone-d_6, 30 °C, 100.13 MHz).

It has been well established that substitution of ligands, slight changes in the coordination geometry, or even isotopic substitution may have an appreciable influence on the transition metal chemical shift of the resulting complexes.[56] The ^{103}Rh NMR of Rh complexes containing coordinated ligands such as C_5H_5, CH_3, or H have only recently been measured,[57,58] and notably such ligands which possess either or both a large σ-donor and π-acceptor capacity give rise to appreciable low-frequency shifts, as compared to *e.g.* Rh−halide or −phosphine complexes.

The ^{103}Rh NMR data for **3** in CD_2Cl_2 are consistent with the presence of a Rh(I) center possessing an approximate trigonal-bipyramidal geometry where the PP_3 ligands takes up one apical and three equivalent equatorial positions and the hydride takes the other apical site. The chemical shift of the Rh nucleus in **3** (δ −1159 ppm) very well fits a description as a Rh(I) compound bearing—apart from the PP_3 ligand—two hydride groups or one hydride and an auride group, since the shift for **3** is found in the range of those observed for dihydrido rhodium species such as $[(PP_3)Rh(H)_2]BF_4$ at −1429 ppm.[59] Complex **4** clearly must have a completely different structure based on its ^{103}Rh chemical shift (δ −487 ppm) as compared to that of **3**. This becomes clear when one compares the chemical shift difference between compounds **1** and **2** on the one hand and the difference between **3** and **4** on the other. When going from PP_3 in **1** (δ −58 ppm) to NP_3 in **2** (δ −266 ppm), a relative shift of −208 ppm is obtained, which for complexes with similar structures can solely be ascribed to the effect of substituting an apical P for an N atom. In the case of **3** and **4**, the difference amounts to +672 ppm, which is a significantly larger and in the opposite direction. Therefore, the basic structures of **3** and **4** must be different. On the basis of the Rh spectra alone, it is difficult to predict the exact structure. Nevertheless, one may argue that the observed relative shift of +672 ppm when going from **3** to **4** must at least partly be ascribed to a change in the formal oxidation number of Rh; *i.e.*, since a shift to higher frequency is observed, **4** should possess formally a Rh(III) center. This would mean that the Rh center in compound **4** is more or less octahedrally surrounded by six donor ligands, whereas for **3** a description as a distorted trigonal-bipyramidal structure is more appropriate.

As has recently been pointed out,[58] correlation of the oxidation state with the chemical shift of rhodium is only of limited value, and this will certainly hold for the case of the present hydride and hydride−auride compounds. As a striking observation, we would like to mention, however, that the gold atom in **3** gives rise to a large low-frequency shift ($\Delta\delta$ −1101 ppm) compared to the parent hydride **1**. This shift must be due to an increase in ΔE term in the Ramsey equation (eq 1)

$$\sigma_p = -\mathrm{cst}(\Delta E)^{-1}\langle r^{-3}\rangle_d$$

and is probably caused by an interplay between the unipositive charge of the now cationic rhodium center and the coordination of gold to Rh. As a result, additional transitions (also Rh to Au) are generated which may tend to increase the average excitation energy ΔE relative to **1** (and **2**). In **4**, this effect is counteracted mainly by the change of coordination geometry toward the octahedron, which will have smaller ligand field splitting than the quasi-trigonal-bipyramidal geometry in **3**.

In conclusion, the ^{103}Rh NMR data do corroborate the ^1H and ^{31}P NMR evidence according to which the structures of **3** and **4** in solution are analogous to those determined in the solid state by X-ray crystallography (*vide supra*).

Attack of $[(XP_3)MY]$ Systems by Electrophiles [X = N, P; M = Co(I), Rh(I), Ir(I)]. In trigonal-bipyramidal complexes of the formula $[(XP_3)MY]$ (X = N, P; M = Co(I), Rh(I), Ir(I); Y = uninegative ligand), the metal is a nucleophilic center susceptible to attack by a plethora of electrophiles.[2-4,20a] However, when the uninegative coligand Y exhibits residual nucleophilic properties as is the case of hydride,[2a,5] cyanide,[3d] and alkynyl[2b,3e,60] groups, electrophiles E^+ may either attack the metal or the coligand. In the latter case, the formal oxidation

(56) (a) Laszlo, P., Ed. *NMR of newly accessible nuclei*; Academic Press: Oxford, U.K., 1983. (b) Pregosin, P. S., Ed. *Transition metal nuclear magnetic resonance*; Elsevier: Amsterdam, The Netherlands, 1991.
(57) (a) Ruiz, J.; Mann, B. E.; Spencer, C. M.; Taylor, B. F.; Maitlis, P. M. *J. Chem. Soc., Dalton Trans.* **1987**, 1963. (b). Duckett, S. B; Haddleton, D. M.; Jackson, S. A.; Perutz, R. N.; Poliakoff, M.; Upmacis, R. K. *Organometallics* **1988**, *7*, 1526. (c) Maurer, E.; Rieker, S.; Schollbach, M.; Schwenk, A.; Egolf, T.; von Philipsborn, W. *Helv. Chim. Acta* **1982**, *65*, 26.
(58) Mann, B. E. In *Transition metal nuclear magnetic resonance*; Pregosin, P. S., Ed; Elsevier: Amsterdam, 1991; p 190.
(59) Peruzzini, M.; Bianchini, C.; Ernsting, J. M.; Elsevier, C. J. Unpublished results.
(60) Bianchini, C.; Meli, A.; Peruzzini, M.; Zanobini, F.; Zanello, P. *Organometallics* **1990**, *9*, 241.

Scheme 2

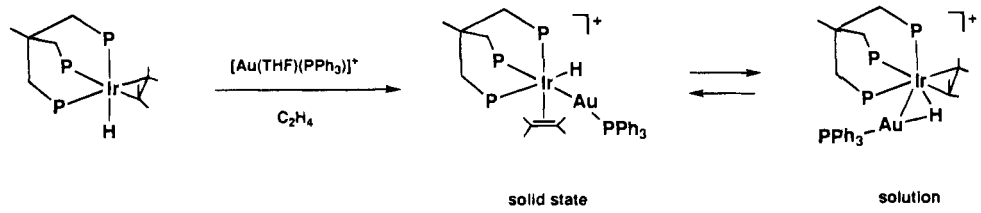

of the Y coligand occurs. The course of the reactions is controlled by the nature of the electrophilic reagent, and for electrophiles of comparable size, the enthalpic contribution generally predominates over the steric one.[3d] When the electrophile directly attacks the coligand Y, the resulting neutral E−Y group may remain coordinated in either η^1 or η^2-fashion. Alternatively, oxidative cleavage of the E−Y bond may occur to give octahedral metal-d^6 complexes. The occurrence of either reaction path depends on a number of factors, which include the nature of the bridgehead donor atom in the tripod and of the metal center. It has also been observed that the structure of the product of electrophilic addition may change on going from solution to solid state.[2e] Illustrative examples of this type of reactivity are the followings.

The cobalt complex $[(PP_3)Co(H_2)]^+$, obtained by protonation of $[(PP_3)CoH]$,[2a] contains an intact dihydrogen ligand in the solid state when the counteranion is BF_4^-, PF_6^-, or $SO_3CF_3^-$, whereas it converts to the Co(III) classical dihydride $[(PP_3)Co(H)_2]^+$ in the solid state when the counteranion is BPh_4^-.[2a,e] In solution it is very likely that the cobalt complex is a classical dihydride,[61] the short T_1 value (19 ms at 203 K in acetone-d_6 at 300 MHz)[2a] being a consequence of the high quadrupole moment of ^{59}Co ($I = {}^7/_2$) and then of the efficient cobalt-hydrogen dipolar interaction which reduces the observed T_1 values.[55]

Upon protonation, the rhodium−NP_3 monohydride **1** is converted to a classical dihydride in both the solid state and solution[5] whereas the protonation product of the PP_3 monohydride **2**, $[(PP_3)RhH_2]^+$, is a dihydride which readily undergoes the reductive coupling of the hydrides in room temperature solutions. The thermal elimination of H_2 was initially ascribed to the existence of an equilibrium between a classical octahedral dihydride and a trigonal-bipyramidal η^2-H_2 complex, the latter predominating at higher temperatures. A recent NMR reinvestigation of the proton and ^{103}Rh spectrum of $[(PP_3)Rh(H)_2]^+$ and of its monodeuterated isotopomer $[(PP_3)Rh(H)D)]^+$ has questioned, in both the solid state and solution, this hypothesis showing that both complexes can be formulated as a classical dihydride and a deuteride−hydride, respectively.[61] Thus the facile elimination of H_2 for the PP_3 complex may be ascribed again to the major propensity of the polyphosphine toward formation of trigonal-pyramidal metal fragments. It is also worth mentioning the reaction between $[(PP_3)RhSH]$ and Me^+ from $MeOSO_2CF_3$ to give $[(PP_3)Rh(H)(SMe)]^+$).[20a] The formation of the Rh(III) hydride−methanethiolate complex has been interpreted in terms of initial electrophilic attack by Me^+ at the hydrosulfide ligand to give rhodium-coordinated MeSH, followed by oxidative cleavage of the S-H bond.[20a]

Prior to the examples described in this paper, no reaction between $Au(PPh_3)^+$ and hydrido metal complexes stabilized by either NP_3 or PP_3 has ever been reported. The closest example is the reaction between $[(triphos)Ir(H)(C_2H_4)]$ and $Au(PPh_3)^+$ illustrated in Scheme 2.[27]

In solution, the iridium center in the resulting mixed-metal complex $[(triphos)Ir\{\eta^2\text{-}HAu(PPh_3)\}(C_2H_4)]^+$ is coordinated to an intact $HAuPPh_3$ unit *via* the Au-H bond. Upon crystallization, breakup of the Au-H bond occurs in the solid state to give $[(triphos)Ir(H)\{Au(PPh_3)\}(C_2H_4)]^+$.

In view of all these literature reports as well as the isolobal analogy between H^+ and $Au(PPh_3)^+$ units,[11] it is very much likely that the $Au(PPh_3)^+$ fragment reacts with the trigonal-bipyramidal monohydrides **1** and **2** *via* direct attack at the terminal hydride ligand. In our opinion, initial electrophilic attack at the hydride rather than at the metal center is favored by the large size of $Au(PPh_3)^+$ that would not find enough room between the equatorial phosphine arms of the tripod ligand where the HOMO is largely developed in trigonal-bipyramidal d^8-metal complexes.[6] Once the $HAuPPh_3$ assembly is formed, oxidative insertion of the metal into the H-Au bond occurs only for the NP_3 complex consistently with the easier propensity of $(NP_3)M$ fragments as compared to $(PP_3)M$ systems to develop the hybridized σ and π FMOs that promote oxidative addition pathways.[6] This ultimately results in formation of more stable octahedral d^6-metal complexes with NP_3 and accounts for the proclivity of analogous PP_3 derivatives to undergo reductive coupling reactions. Within this context, it is reasonable to conclude that the elimination of H_2 from $[(PP_3)Rh(H)_2]^+$ may occur via a trigonal-bipyramidal η^2-H_2 intermediate or transition state.

Acknowledgment. Thanks are due to Mr. Dante Masi and Mr. Paolo Innocenti for technical assistance. Thanks are also expressed to EC for financial support (contract No. CHRX-CT930147).

Supplementary Material Available: Tables of final positional parameters and U values for all atoms of **3b** and **4** (8 pages). Ordering information is given at any current masthead page.

(61) (a) $^1H\{^{31}P\}$ NMR spectroscopy (21 °C, acetone-d_6, 200.13 MHz) reveals that $[(PP_3)Rh(H)(D)]^+$ exhibits a narrow doublet at δ −7.068 [$\Delta_\delta = \delta_{H2} - \delta_{HD} = 205$ ppb] with ^1J(HRh) 15.1 Hz. $^1H\{^{103}Rh\}$ NMR (acetone-d_6, 100.13 MHz) gave δ −1429 (at 30 °C) and δ −1463 (at −90 °C), which points to the presence of Rh−dihydride species at high as well as at low temperature. $^1H\{^{31}P\}$ NMR experiment carried out on a solution of $[(PP_3)Co(H)(D)]^+$ shows a broad unresolved resonance (21 °C, acetone-d_6, 200.13 MHz) centered at δ −10.736 [$\Delta_\delta = \delta_{H2} - \delta_{HD} = 184$ ppb] with no discernible ^1J(HD). A full account of these measurements which clearly confirm the classic nature of the $[(PP_3)MH_2]^+$ complex cations will be published in due time. (b) Similar results have been obtained by D. M. Heineckey, personal communication.

(62) Casalnuovo, A. L.; Laska, T.; Nilsson, P. V.; Olofson, J.; Pignolet, L. H. *Inorg. Chem.* **1985**, *24*, 233.

(63) Luke, M. A.; Mingos, D. M. P.; Sherman, D. J.; Wardle, R. W. M. *Transition Met. Chem.* **1987**, *12*, 37.

(64) Douglas, G.; Jennings, M. C.; Manojlovic-Muir, L.; Puddephatt, R. J. *Inorg. Chem.* **1988**, *27*, 4516.